Automatic Measurement of Atrophy Rates in Hippocampal Subfields from Longitudinal High-Resolution T2-weighted MRI

S. Das[1], B. Avants[1], J. Pluta[1], C. Craige[1], M. Weiner[2], S. Mueller[2], and P. Yushkevich[1]
[1]PICSL, Department of Radiology, University of Pennsylvania, Philadelphia, PA, United States, [2]VA Medical Center, University of California at San Francisco, San Francisco, CA, United States

Introduction

We present the first study to attempt measurements of longitudinal atrophy rates within hippocampal subfields from in vivo T2-weighted MRI. MRI-based focal measurements of longitudinal change within subfields of the hippocampal formation (HF) have great potential clinical value as biomarkers of disease progression in neurological disorders such as Alzheimer's disease (AD), as pathology studies have shown that subfields are differentially affected at certain stages of the disease process, and can undergo pathological changes at differing rates. However, commonly acquired T1-weighted 1x1x1mm^3 structural MRI does not have sufficient intensity contrast to reliably distinguish subfields and make such measurements. Thus, focal T2-weighted MRI designed for imaging the HF (HF-MRI) has emerged as a useful modality for making subfield-specific volumetric measurements [1,2]. Yet, longitudinal change measurements from these images have not yet been attempted, partly because of the methodological challenges associated with analyzing these images. We propose a method that uses a combination of existing techniques adapted to address these difficulties to measure longitudinal change within subfields. We evaluate our method in a repeat scan dataset and show that atrophy patterns consistent with known pathology can be detected in a cohort of cognitively impaired patients.

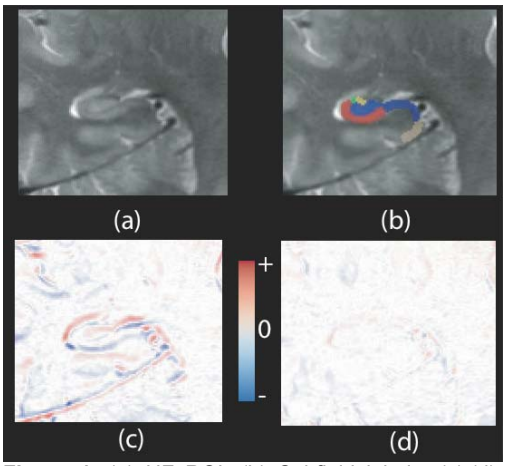

Figure 1: (a) HF ROI, (b) Subfield labels, (c),(d): Difference image after global alignment using whole brain and ROI-based registration, respectively. White indicates better alignment.

Methods

Imaging: Subjects included 11 patients (age 71.5±6.5 yrs), 5 diagnosed with mild cognitive impairment (MCI), and 6 cognitive impaired, but not meeting clinical criterion for MCI, and 6 age-matched healthy elderly controls (age 70.2±6.9 yrs). Images were acquired on a Bruker MedSpec 4T system controlled by a Siemens Trio^{TM} console using a USA instruments 8 channel array coil consisting of a separate transmit coil enclosing the receiver coils. Two types of MRI were acquired: 1) 3D T1-weighted MRI (MPRAGE) with TR/TE/TI=2300/3/950 ms, 7^0 flip angle, 1.0 mm isotropic resolution, FOV 256x256x176, 2) T2-weighted images with fast spin echo sequence (TR/TE: 3990/21 ms, echo train length 15, 18.6 ms echo spacing, 149^0 flip angle, 100% oversampling in ky direction, 0.4x0.4 mm in plane resolution, 2 mm slice thickness, 24 interleaved slices without gap, angulated perpendicular to the long axis of the hippocampal formation) (Fig. 1). Followup scans were obtained one year after the baseline scans. In a separate test-retest cohort of 9 healthy controls (age 42.2±16.3 yrs), two sets of scans were obtained on the same day, with slightly different head positions in the scanner.

Longitudinal Image processing: Our method addresses the challenges posed by HF-MRI in each analysis step as follows: 1) First, the baseline (BL) and followup (FU) images are brought into global alignment using the FLIRT tool [3]. The highly anisotropic voxel size makes whole brain registration suboptimal for accurate alignment of the HF ROI. Instead, we define an HF ROI based on a mask of HF and separately register left and right ROIs, after an initial alignment using the T1-weighted images. Fig. 1 shows that ROI-based registration is more accurate than whole brain registration. 2) Deformable registration (using ANTS [5]) between the globally aligned pair of images provides measurement of local volume change. Following [4], we ensure unbiased measurements by applying the global transformation symmetrically to both BL and FU images so that they undergo similar amounts of global transformation and the same number of resampling operations. Further, the similarity metric is computed in a neutral halfway space. 3) Out-of-slice deformations can lead to severe aliasing, and within-slice deformations are more reliable in HF-MRI because of high in-slice resolution and thick slices. Therefore, instead of 3D registration, we use 2D deformable registration between corresponding slices in the globally aligned image pair. 4) The baseline HF-MRI images are segmented into 9 ROIs over which longitudinal changes are measured: CA1, CA2, CA3, dentate gyrus (DG), HEAD, TAIL, subiculum (SUB), entorhinal cortex (ERC) and parahippocampal gyrus (PHG), and whole hippocampus (HIPP) as described in [2]. Integrating the Jacobian determinant of the deformable transformation over each ROI label gives a measure of change in the ROI.

ROI	Patients			Controls			Test-retest	
	U	B	M	U	B	M	U	B
CA1	**1.1±1.1**	**1.7±1.1**	**5.6±7.2**	0.1±0.8	0.6±0.8	2.8±4.2	0.2±0.6	**0.6±0.7**
CA2	0.6±2.0	**2.0±1.8**	3.4±10	-0.8±2.2	0.8±1.3	-3.5±6.5	0.5±2.1	1.6±2.2
CA3	0.4±2.5	**1.8±2.3**	**5.6±7.7**	-0.8±1.4	**2.1±1.4**	1.2±18.3	1.1±1.7	**1.5±1.5**
DG	**1.9±2.0**	**3.1±2.0**	**5.2±7.8**	0.8±2.2	**1.1±2.5**	-0.9±3.8	0.4±1.4	1.2±1.8
HEAD	**1.0±1.0**	**1.7±1.1**	5.2±3.2	0.1±0.7	**0.7±0.6**	1.2±6.6	0.2±0.6	**0.6±0.5**
TAIL	**1.2±1.8**	**2.5±1.6**	1.7±6.9	0.0±1.2	**1.7±1.3**	-3.2±3.9	0.2±1.4	**1.0±1.2**
SUB	0.8±1.8	0.7±2.0	2.0±12	**0.8±0.8**	**0.9±1.1**	3.5±12.7	0.4±1.5	**1.3±1.5**
ERC	**1.3±1.3**	**3.6±1.5**	2.8±8.5	0.5±2.7	**2.4±2.8**	-4.1±8.6	-0.1±1.7	**2.1±1.7**
PHG	**0.8±1.2**	**2.4±1.5**	-5.3±10	-0.1±1.5	**1.5±1.5**	4.2±16.6	-0.1±2.0	**1.2±1.7**
HIPP	**1.0±1.0**	**1.8±1.1**	1.3±2.4	0.1±0.7	**0.9±0.6**	1.2±5.4	0.2±0.7	**0.9±0.7**

Table 1: Yearly atrophy rate, averaged over left and right, as percent change: mean±std dev. U= proposed unbiased method, B=biased and M=manual method. Positive: volume decrease, Bold: significant at p<0.05, Red: Patients > controls at p<0.05.

Results

Results of longitudinal measurements are given in Table 1. The U columns show measurements using the proposed unbiased method. In the test-retest dataset, where repeat scans were treated as followup, no significant change was found in any ROI, as expected. In the longitudinal cohort, significant change was detected in the patient group in several subfields, including CA1 and HEAD, as well as HIPP. Patients also showed significantly greater atrophy rate than controls in CA1, HEAD and HIPP. Note that independent manual segmentations (M columns) produce highly variable measurements with unrealistic atrophy rate estimates. In a separate experiment, we used a traditional, asymmetric deformable registration framework that resamples only the FU image and computes the similarity metric in the BL image space (B columns in Table 1, biased method). This led to a positive bias in the measurements, similar to bias in whole hippocampus atrophy rate estimates from isotropic T1-weighted MRI [4], as evidenced by significant change being detected in the test-retest data.

Discussion

To our knowledge, this is the first study to attempt longitudinal atrophy rate measurements in hippocampal subfields. We identify the methodological challenges of making accurate longitudinal measurements from anisotropic HF-MRI data, and propose potential solutions to address them. Our method does not detect change in test-retest data, but finds atrophy in subfields such as CA1 in patients, consistent with literature [1]. These are preliminary findings, and a larger dataset will be necessary for further evaluation and drawing more clinically meaningful conclusions. Nonetheless, current results are promising, and may lead to development of subfield-specific MRI-based longitudinal biomarkers of disorders such as Alzheimer's disease.

References: [1] Mueller SG et al., Hum Brain Mapp, 31(9),1339–47, 2010. [2] Yushkevich PA et al., Neuroimage, *in press*. [3] Smith, SM et al., Neuroimage, 23(S1), 208–19, 2004. [4] Yushkevich et al., Neuroimage, 50(2), 434–45, 2010. [5] Avants BB et al., Med Image Anal, 12(1), 26–41, 2008.
Acknowledgements: Penn-Pfizer Alliance grant 10295 and NIH grants K25 AG027785, R21 NS061111, and R01 AG010798.